hemerythrin.[5] Of the five histidine imidazole ligands to the binuclear iron cluster in hemerythrin, two are trans and three are cis to the μ-oxo bridge.[41] The structure of highest resolution, that of azidometmyohemerythrin,[41b] shows that all three cis Fe–N_{Im} bond distances are more than 0.1 Å shorter than the two trans Fe–N_{Im} distances. μ-Sulfidomethemerythrin shows only two closely spaced N–H resonances (at 25 and 23 ppm),[5] consistent with the relatively smaller trans effect expected for a μ-sulfido bridge.

The best signature for a μ-hydroxo-bridged diiron(III) site in protein spectra may be histidyl ligand β-CH_2 resonances at $\sim$ 15–17 ppm, judging from the positions of the N–CH_3 resonances of $[Fe_2(OH)(O_2CMe)_2(TMIP)_2]^{3+}$ and $[Fe_2(OH)(O_2CEt)_2(TMIP)_2]^{3+}$ (Figure 6B).

(41) (a) Stenkamp, R. E.; Sieker, L. C.; Jensen, L. H. *J. Am. Chem. Soc.* **1984**, *106*, 618–622. (b) Sheriff, S.; Hendrickson, W. A.; Smith, J. L. *J. Mol. Biol.* **1987**, *197*, 273–296.

Mixed-Valent "Basic Iron Carboxylate" Clusters. All imidazole ring positions are observable. Because of valence delocalization, the opposing dipolar (upfield) and contact (downfield) contributions to the isotropic shifts can be understood by considering orientations and distances of the ligand protons with respect to the magnetic axes of the *cluster*.

Note Added in Proof. The X-ray crystal structure of $[Fe_2O(O_2CMe)(TMIP)_2](ClO_4)_2$ (Wu, F.-J.; Hagen, K. S.; Kurtz, D. M., Jr., unpublished results) shows that the two trans Fe–N_{Im} distances are an average of 0.03 Å longer than the four cis Fe–N_{Im} distances.

Acknowledgment. We thank Dr. Sergiu Gorun for a gift of TICOH, Jihu Zhang for experimental assistance, and Professor Larry Que, Jr., for helpful discussions. This research was supported by NIH Grant GM 37851 (D.M.K.). D.M.K. is an NIH Research Career Development Awardee.

Deuterium Isotope Effects on Carbon-13 NMR Shifts and the Tautomeric Equilibrium in *N*-Substituted Pyridyl Derivatives of Piroxicam

Jon Bordner, Philip D. Hammen, and Earl B. Whipple*

Contribution from Pfizer Inc., Central Research, Groton, Connecticut 06340.
Received January 5, 1989

Abstract: *N*-Alkylated pyridyl derivatives of piroxicam are formally zwitterionic but can, at the expense of aromaticity in the pyridyl ring, revert to neutral structures by means of fast internal proton transfers. The large change in dipole moment accompanying these tautomeric shifts makes the equilibrium unusually sensitive to changes in chemical substitution, solvent, and temperature. This property is used to formulate, test, and verify a new type of deuterium isotope effect on carbon-13 NMR shifts recently proposed by Hansen and, in the process, establish close correspondence with the general theory of isotope effects on proton transfer equilibria.

1. Introduction

In addition to being an important article of commerce as a nonsteroidal antiinflammatory agent,[1] piroxicam (Feldene) is an intrinsically interesting chemical compound by virtue of possessing four different heteroatom sites for positioning the two substituents necessary to complete its partial structure shown in Figure 1. Twelve isomers are possible if the substituents are nonidentical, and several have been prepared.[2] These differ remarkably in properties, particularly if substitution occurs on the pyridyl nitrogen to present the system with the formal alternatives of charge separation or bond localization in the pyridyl ring. Nevertheless, such substitution occurs with surprising ease.[2] When the amide nitrogen is also substituted, its fully valence-bonded structures are necessarily zwitterionic; yet piroxicam itself has been shown to crystallize in this form.[3] There is also, within the manifold of near-planar arrangements (which generally occur if one of the substituents is hydrogen), a total of eight possible geometrical isomers about the three partial double bonds connecting the two ring systems, and four of these arrangements (the 9,10 bond is consistently *Z*) have been found.

Piroxicam. The parent compound in which both substituents are hydrogen crystallizes in two forms, one of which has the initially proposed 7,10 *EZE* structure, **1a**,[4] and the other is a crystal hydrate of the zwitterionic 10,16 *ZZZ* form, **1b**.[3] It was

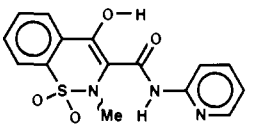

1a

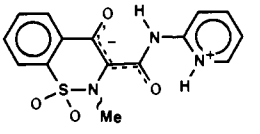

1b

recently demonstrated that the zwitterion coexists in equilibrium with the neutral form to the extent of 19% in *N*,*N*'-dimethylformamide (DMF) at 205 K, and the situation can be roughly extrapolated to include other polar solvents (e.g., DMSO) at ambient temperature.[5]

Monoalkyl Derivatives. The original attempts at *O*-methylation of piroxicam led instead to the *N*-methylated pyridyl derivative, and a series of *N*-alkyl homologs have since been reported.[2] Their physical properties (high melting points, yellow color, and low solubility) resemble zwitterionic piroxicam, and the crystal

(1) Lombardino, J. G.; Wiseman, E. H. *Med. Res. Rev.* **1982**, *2*, 127.
(2) Hammen, P. D.; Berke, H.; Bordner, J.; Braisted, A. C.; Lombardino, J. G.; Whipple, E. B. *J. Heterocycl. Chem.* **1989**, *26*, 11.
(3) Bordner, J.; Richards, J. A.; Weeks, P.; Whipple, E. B. *Acta Crystallogr.* **1984**, *C40*, 989.
(4) Kojic-Prodic, B.; Ruzic-Toros, Z. *Acta Crystallogr.* **1982**, *B38*, 2948.
(5) Geckle, J. M.; Rescek, D. M.; Whipple, E. B. *Magn. Reson. Chem.* **1989**, *27*, 150.

0002-7863/89/1511-6572$01.50/0

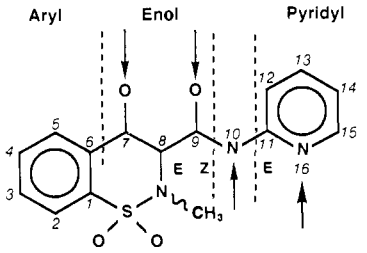

Figure 1. Piroxicam system diagram and positional notation. The planar configuration shown is *EZE*, from left to right.

structure of the *n*-hexyl derivative establishes their 10,16′ *ZZE* structure, **2b**, which differs from **1b** only by a 180° rotation of the pyridyl ring that provides an additional internal hydrogen bond in piroxicam.

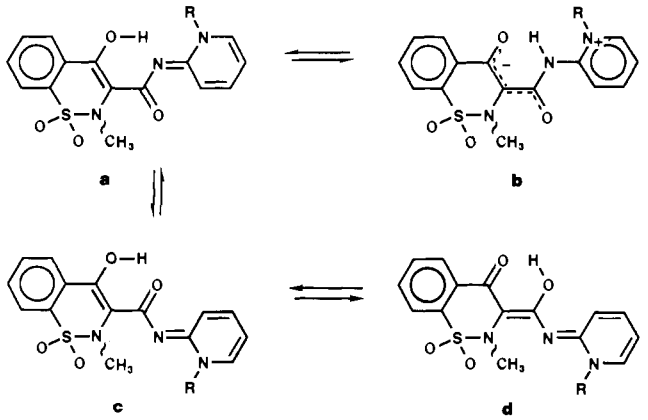

2a-2d (R = $-CH_3$)
2a′-2d′ (R = $-CH(CH_3)OCOOC_2H_5$)
2a″-2d″ (R = n-hexyl)

A series of *O*-alkyl homologs was also reported, their 7,10 *ZZE* form proved by the crystal structure of one member and the ^{13}C and ^1H NMR spectra of both series assigned.[2]

Enolate. In the course of investigating the zwitterionization of piroxicam in solution,[5] we also had occasion to assign the NMR spectrum of its enolate. Its crystal structure, in the form of an ethanolamine salt, was independently determined and is described in section 6. It has the expected 10 *ZZE* structure.

2. *N*-(α-Diethyl carbonate) Derivative

Although this *N*-substituted pyridyl (R = $-CH(CH_3)-OCOOC_2H_5$) derivative of piroxicam, which also occurs as a minor byproduct of *O*-substitution, has the same fixed structure as the *N*-alkyl series mentioned above,[2] it is highly soluble in both polar and nonpolar solvents, and its NMR shifts do not correspond to those measured in the prior series.[2] The NMR spectrum in chloroform solution at room temperature contains several broadened lines, while that in dimethyl sulfoxide is fairly sharp. On cooling, the spectrum in chloroform solution first splits (at 250 K) into two resolved components, and subsequently (at 220 K) into four. The ratio of the principal forms is about 4/3 at 250 K, but extrapolation of the measured intensities over the range 215–255 K indicates that the minor form predominates at ambient temperature. The chemical shifts assigned to the minor low-temperature form (column 4 of Table I) also correspond more closely to those in the ambient temperature spectrum in $CDCl_3$ solution.

The totally averaged spectrum at room temperature was assigned rather straightforwardly, first by grouping the two sets of coupled protons into sequences based on $^3J(H,H)$ coupling constants and then by assigning the pyridyl ring sequence (and confirming the position of the side chain) by means of a nuclear Overhauser enhancement of H15 by the doublet methyl protons. A ^{13}C, ^1H shift correlation experiment[6] then assigned the protonated pyridyl ring carbons and inversely served to assign the protons on the aryl ring, since the ^{13}C shifts in this region of the molecule are identifiable by comparison to prior models.[2] Selective $^{13}C\{^1H\}$ decoupling experiments were used to assign the non-protonated carbons as follows: (1) C1 by strong coupling to H5 and C8 by weak coupling to the sulfonamide methyl protons; (2) C11 and C9 through nuclear Overhauser polarizations by H12 and the sulfonamide methyl protons, respectively; and (3) C6 and C7 on the basis of their very different chemical shifts.

Each of the NMR signals is split into as many as four components at 220 K, which can be traced to the assigned position in the averaged spectrum through observation of its variable temperature behavior, first through a coalescence of secondary pairs into two primary species at 250 K and followed by the coalescence of the primary pairs near room temperature. The intensity ratio of the two primary forms, as measured from their enol proton signals, is too near unity to allow the carbon-13 spectrum to be differentiated by species on this basis, but a more significant difference (1.7 vs 5.4) occurs in the relative intensities of the secondary pairs. The latter is sufficient to allow the identification of several ^{13}C resonances (positions 9, 7, and 11) for which all four components are resolved at 220 K with the corresponding enol proton line, and, somewhat less certainly, two additional sets (positions 6 and 8) where only one principal line splits into secondary components. The difference in secondary intensity ratios can also be used to assign the pyridyl ring protons, since H12 shows partially resolved bands from all four forms, and

Table I. Carbon-13 Shifts in Compound **2′**[a]

		chloroform-*d* solution			
position[b]	solid δ_s	298 (K) ≪δ≫	220 (K) δ_1[c,d]	250 (K) ⟨δ⟩	220 (K) δ_2[c,e]
9	175.2	175	174.70	←175.00	168.54
			174.84	168.87→	169.35
7	157.4	158.0	157.69	157.87→	158.88
			157.60	←157.72	157.51
11	155	156.2	156.23	←156.13	153.81
			155.86	154.46→	154.77
19	152.2	152.6	152.34	152.23	152.29
			152.07		
13	142.4	141.2	141.13	141.93→	142.23
			141.42	←140.88	
1	133.7	135.3		134.41	
				134.33	
15		132.6	132.5u	←132.44	132.5u
				132.21→	
4		132.2	132.5u	132.21	132.5u
3		131.2	131.3u	131.13	131.3u
6		130.2	129.17	130.26→	130.35
				←129.29	130.09
5	125.0	126.2		126.19	
				125.76	
2	122.6	123.5		123.36	
12	119.8	121.1	120.81	←120.77	120.51
				120.64→	
8		116.3	115.56	←115.74	114.75
				115.25→	115.20
14	114.1	114.0	114.16	115.40→	115.99
			114.43	←113.77	115.81
17	80.9	81.1	80.38	80.78→	80.88
				←80.52	80.52
21	64.9	65.5		65.77	
				65.31	
8″	38.4	38.5	38.53	←38.48	38.34
				38.07→	38.17
17′	19.8	20.5	20.84	←20.66	20.33
			21.00	20.38→	20.93
22	14.0	14.1		14.00	

[a] Measured at 62.87 MHz. [b] See Figure 1. The side-chain atoms are numbered in outward order, beginning with C17 attached to N16 in the pyridyl ring. [c] Duplicate column entrys listed downward in order of decreasing intensity. [d] Predominantly tautomer **2c′**. [e] *ZZE* rotamer, principally in tautomeric form **2a′**, as discussed in text.

(6) Bax, A.; Morris, G. *J. Magn. Reson.* **1981**, *42*, 501.

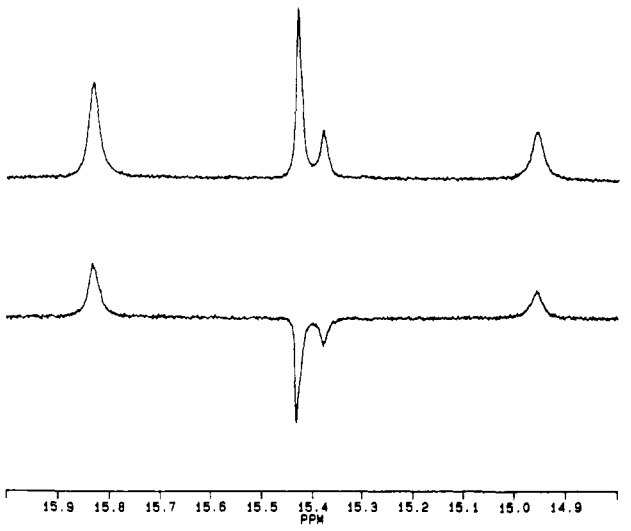

Figure 2. Enol proton spectrum of compound **2′** in $CDCl_3$ solution at 220 K. The lower trace, observed 0.5 s following a 180 K inversion pulse, demonstrates the differing relaxation times of the two primary pairs of lowest temperature components.

the low-temperature COSY[7] spectrum serves to assign all the rest. The sulfonamide and 17′-methyl proton resonances are also assignable on the basis of their intensity distribution. With the protons thus assigned to individual components, their attached ^{13}C signals were included by heteronuclear shift correlation in two dimensions. One can thus make the species specific assignments listed in Table I to most of the NMR spectrum, based originally on the intensity distribution of the enol proton lines.

A single crystal grown inadvertently from dimethyl sulfoxide solution was found (section 5) to consist of the 7,16′ *EZE*(*RS*/*SR*) structure, **2c′**. The powder diffraction pattern calculated from the single-crystal data matches that of the material used in our NMR experiments, and the CP/MAS carbon-13 spectrum of this powder, in addition to correlating generally (Table I) with the spectrum observed in chloroform solution, contains the unique (among all known derivatives of piroxicam) 175 ppm line assigned to C9 in the spectrum of the less abundant primary form at 250 K, allowing one to identify the spectrum in column 4 of Table I with this structure.

In the enol proton spectrum in Figure 2, the members of each secondary pair have equal relaxation times, but that now identified with the 7,16′ *EZE* form has significantly longer (1.7 s vs 0.4 s at 220 K) T_1's than those from the other. The source of the shorter T_1's was traced by homonuclear NOE difference measurements to the protons near the beginning of the pyridyl side chain, thus serving to establish the geometry of both secondary members of the primary form in column 6 of Table I as *ZZE*.

Having thus identified the primary forms as *EZE* and *ZZE* rotamers, the most plausible explanation of the secondary process is the presence of a chiral center in the side chain, which upon the arrest of sulfonamide *N*-inversion, gives diastereomers. The coalescence temperature of the secondary process, unlike the first, is rather insensitive to change of solvent or to the rotameric form. The larger effect on the secondary equilibrium populations occurs in the *EZE* rotamer where the chiral atoms are closest together, while the larger differences in chemical shift occur in the enol region of the *ZZE* rotamer, which is close to the side chain. While interesting in its own right, the secondary process thus becomes incidental with the main concerns of the present study, except to indicate that both rate processes are intrinsic to the piroxicam system itself and not the side chain. We have not yet obtained a similar, nonchiral compound which would both prove this secondary issue and greatly simplify the spectra.

To our initial surprise, the chemical shifts thus assigned to the *ZZE* form of **2′** do not match those of the *N*-alkylated forms of

(7) Aue, W. P.; Bartholdi, E.; Ernst, R. R. *J. Chem. Phys.* **1976**, *64*, 2229.

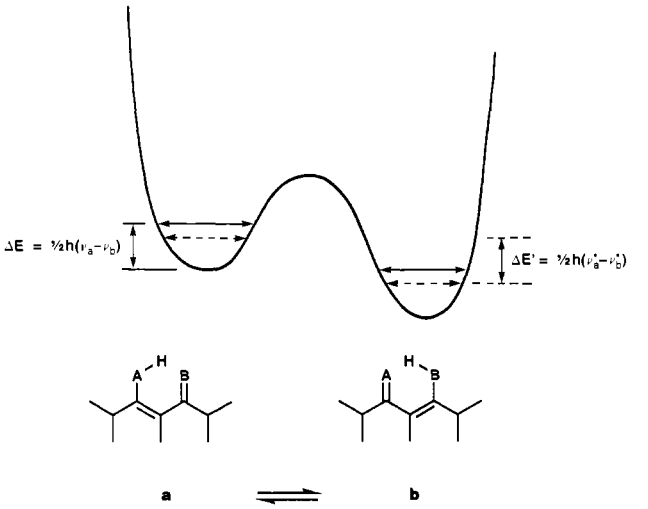

Figure 3. Sketch of the double minimum for proton stretching.

piroxicam[2] well enough to permit the assertion that their structures are the same. To resolve this dilemma, one has to propose that the position of the fast tautomeric equilibrium between the 7,16′ and 10,16′ *ZZE* forms, **2a′** and **2b′**, is shifted substantially to the left. This is plausible on the basis of an inductive polarization of C17 by the carbonate function, causing it to oppose zwitterionic charge on the pyridyl nitrogen. We therefore infer that compound **2′** in chloroform solution consists of mainly of a mixture of formally neutral 7,16′ *EZE* and *ZZE* forms, **2a′** and **2c′**, while the *N*-alkyl derivatives have the formally zwitterionic 10,16′ *ZZE* structure, **2b**.

3. Carbon-13 Isotope Shifts

It has been proposed that deuterium isotope shifts in the ^{13}C NMR spectra of systems of the general form A ⇌ B in Figure 3 reflect, especially when observed at positions remote from the site of substitution, a perturbation of the fast equilibrium between the tautomeric forms.[9] This would amount to a third general class of isotope shift, appended to the localized perturbation of the vibrational averaging of chemical shift tensors, or over longer ranges to the lifting of degeneracy in double minima.[10]

Denoting the deuterated species by primes, the averaged shifts in a two component system p and q are given by

$$\Delta\delta_i \equiv \delta_i - \delta_i' = x_p\delta_{ip} + x_q\delta_{iq} - x_p'\delta_{ip}' - x_q'\delta_{iq}' = \delta_{iq} - \delta_{iq}' + x(\delta_{ip} - \delta_{iq}) - x'(\delta_{ip}' - \delta_{iq}') \quad (1)$$

where the mole fractions are designated by

$$x \equiv x_p = 1 - x_q, \qquad x' \equiv x_p' = 1 - x_q'$$

The isotope shifts consist in part of direct perturbations of the vibrational averaging of shielding tensors. Designating these localized terms by λ_i, we have

$$\delta_{ip}' = \delta_{ip} + \lambda_{ip}, \qquad \delta_{iq}' = \delta_{iq} + \lambda_{iq} \quad (2)$$

which on inserting into [1], gives

$$\Delta\delta_i = (\delta_{ip} - \delta_{iq})(x - x') - (x_p'\lambda_{ip} + x_q'\lambda_{iq}) \quad (3)$$

The second term in (3) contains the direct effect of isotopic substitution on the averaged shielding tensors. The λ_i are usually small, negative, and localized over ranges two (~0.1 ppm) to three (~0.5 ppm) bonds removed from the deuteron.[10]

Measured ^{13}C isotope shifts for several piroxicam derivatives are shown in Figure 4. While the *O*-alkyl derivative **3** shows typical localized shifts, those in the *N*-alkylated derivatives **2** and **2′** are larger, of variable sign, and more remotely distributed. The same trend, attenuated several fold, is observed in the enolate **4**.

(8) Willem, R. *Prog. NMR Spectrosc.* **1987**, *20*, 1.
(9) Hansen, P. E.; Duus, F.; Schmitt, P. *Org. Magn. Reson.* **1982**, *18*, 58.
(10) Hansen, P. E. *Prog. NMR Spectrosc.* **1988**, *20*, 207.

Table II. Carbon-13 Chemical Shifts and ^2H Isotope Shifts in *ZZE* Rotamers of N16-Substituted Piroxicams at 220 K[a]

	δ^b							
	2a′				**2b**		**2a**	
position	($CDCl_3$)	(DMF)	**2b**/(DMF)	$\delta_{2b} - \delta_{2a'}$	$\Delta\delta$	$\Delta\delta/(\delta_{2b} - \delta_{2a'})$	$\Delta\delta$	$\Delta\delta/(\delta_{2b} - \delta_{2a'})$
1	134.0	135.3	136.3	2.3	−0.10	−0.043		
2	123.5	123.4	123.7	0.2	±0.02			
3	131.3	131.2	131.9	0.6	0.05			
4	132.5	132.4	133.1	0.6	±0.03			
5	125.8	126.2	127.9	2.1	−0.08	−0.038		
6	130.3	132.1	134.8	4.5	−0.33	−0.073	0.13	0.029
7	158.1	161.2	167.7	9.6	−0.62	−0.064	0.78	0.081
8	114.9	114.4	111.0	−3.9	0.44	−0.113	−0.23	0.059
9	168.8	167.5	165.1	−3.7	0.52	−0.141	0	0
11	154.2	153.4	151.6	−2.6	0.38	−0.146	−0.27	0.104
12	120.5	119.6	117.4	−3.1	0.21	−0.068		
13	142.3	144.3	144.3	2.0	−0.09	−0.045		
14	115.9	117.4	117.3	1.4	−0.13	−0.093		
15	132.5	135.9	143.3	n/a				

[a] Data in column 2 obtained at 62.8 MHz, all other at 126 MHz. [b] Weighted average of secondary forms.

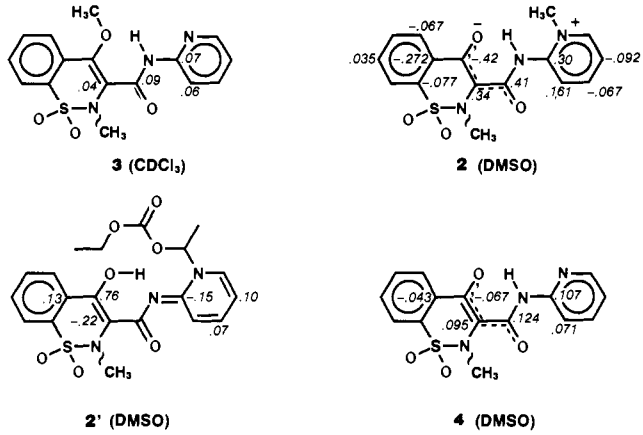

Figure 4. Room temperature isotope shifts.

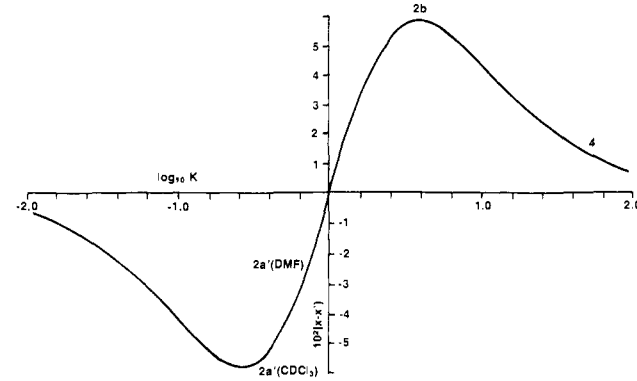

Figure 5. Plot of (8) for the theoretical value of $\alpha = 0.293$. The estimated locations of the several systems described in the text are indicated on the curve.

Most notably, the isotope shifts in **2′** are consistently opposite in sign from those of the *N*-methyl derivative **2**. A general reversal of sign would occur in the first term of (3) on reversal of the direction of equilibrium, since the isotope effect on the equilibrium populations is generally to enhance the normal preference.[11] In order to obtain a general sign reversal from the second term of (3), each pair of localized contributions, λ_{ip} and λ_{iq}, would have to have opposite signs. The first term in (3) also depends on the coefficients $(\delta_{ip} - \delta_{iq})$, which can vary in magnitude and sign.

Hansen's proposal is stated in general enough form to encompass both of the terms in (3). As applied to the first, it can be reduced to the statement that the isotope effect on the free energy difference of the general tautomeric equilibrium A ⇌ B in Figure 3 is proportional to that difference, which is a well-known consequence of the lowering of zero-point vibrational energies by the isotopic mass.[11] If the isotope effect on the equilibrium is represented by Δf, where

$$\Delta F' = \Delta F + \Delta f$$

and we assume as proposed that $\Delta f = \alpha(\Delta F)$, then the equilibrium constants

$$K = x_q/x_p = (1 - x)/x \quad \text{and} \quad K' = (1 - x')/x'$$

are related by

$$K' = K^{1+\alpha} \tag{4}$$

which on insertion into (3), gives

$$\Delta\delta_i + (x_p'\lambda_{ip} + x_q'\lambda_{iq}) = (\delta_{ip} - \delta_{iq})[(K + 1)^{-1} - (K^{1+\alpha} + 1)^{-1}] \tag{5}$$

The general form of this function, sketched in Figure 5, is odd about the origin ($K = 1$) on a logarithmic scale, slowly vanishing in the wings, and reaching extrema in the vicinity of $\log K = \pm 0.6$, whose abscissas are not highly sensitive to the value of α.

The isotope shifts in **2** and **2′** in Figure 4 are both averaged over an incompletely known mixture of *EZE* and *ZZE* forms. This difficulty can be partially overcome, in solvents with low freezing points, by measurements below the coalescence temperature of the rotamers. However, in the case of structure **2′**, each ^{13}C line is split into up to eight components in a mixture of ^1H and ^2H substituted isotopomers, which makes it all but impossible to resolve many of the smaller shifts outside the immediate region of its enolic system. While hence incomplete, the data in Figure 6 nonetheless lead to the following conclusions. First, the similarity of isotope shifts between the two rotamers of **2′** in chloroform solution is general enough to imply that their tautomeric forms are essentially the same; i.e., the 7,16′ form established by the crystal structure of **2c′**. Secondly, the isotope shifts thus identified with structure **2a′** change in the direction of the 10,16′ tautomer, exemplified by **2b**, as the solvent polarity increases.[12] Third and finally, if the chemical shifts in the tautomers **2a** and **2b** are approximated from the spectra associated with forms **2a′**($CDCl_3$) and **2b**(DMF) in Figure 6, then the observed isotope shifts correlate consistently in sign, and roughly in magnitude (Table II), with the coefficients $(\delta_{iq} - \delta_{ip})$ thus estimated. The average value of $x - x'$ obtained from the eight positions in **2b** whose chemical shifts differ by more than 1 ppm, and excluding positions 9–11 where the λ_i are presumably large, is −0.067 ± 0.020. The sign obtained for $(x - x')$ is consistent

(11) Bell, R. P. *The Proton in Chemistry*; Cornell University Press: Ithaca, NY, 1959; Chapter XI.

(12) The conformation of the polar side chain also affects the tautomeric equilibrium, as exemplified by the fact that the isotope shifts in the minor diastereomer of **2a′**($CDCl_3$) are consistently larger by about 20% than those given in Figure 6 for the major diastereomer.

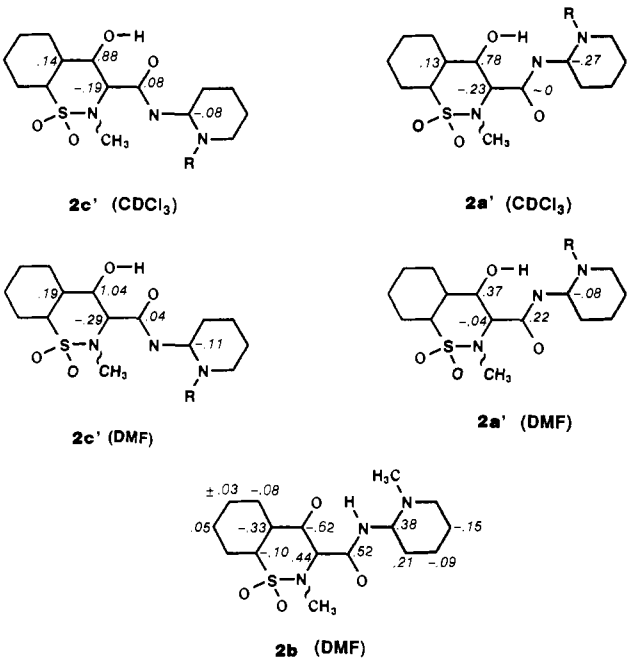

Figure 6. Low-temperature (220 K) isotope shifts. The diagrams and labels represent the predominant tautomer in the rapidly averaged pair. Double bonds and charges are omitted from the diagrams in order to improve the clarity of the data.

with the presumption that the equilibrium in **2a'** is to the left, and **2b** to the right, of Figure 5.

The data as a whole suggest that the equilibria in both **2'** and **2** are in fact near the two extrema of Figure 5, rather than at its wings. The effect of increasing solvent polarity ($CDCl_3$ < DMF < DMSO) and decreasing temperature is predictably[5] to shift points to the right, toward the zwitterion. The sharp decrease in magnitudes of the isotope shifts in the *ZZE* form of **2'** in DMF solution (Figure 6) suggests that this point is between the extrema and slightly to the left of the origin of Figure 5. Two independent estimates, based on interpolation of either its isotope effects or chemical shifts between those in the samples loosely identified as forms **2a'**($CDCl_3$) and **2b**(DMF) in Figure 6, agree that the solvent effect on **2a'** amounts to about 0.3 units in log *K*, which places its chloroform solution near the minimum of Figure 5. The roughly equal and opposite isotope shifts in **2a'**($CDCl_3$) and **2b**-(DMF) then imply, according to the symmetry of the general curve, that **2b**(DMF) is close to its maximum. The improved solubility of the *n*-hexyl homolog,[2] 2'', permits a direct test of this assertion. In DMF solution at 220 K, its isotope shifts correspond closely to those in **2** and change only slightly in methylene chloride or chloroform. In the latter two solvents, the temperature dependence of the isotope shifts can be observed over a fairly wide range, three representative examples being shown in Figure 7.[13] Allowing for the expected discontinuities at the change of solvent, the results, when appropriately scaled, reflect the general shape of Figure 5 in the region of its maximum.

Relocating **2a'**($CDCl_3$) and **2b** in Figure 6 near the extrema rather than the wings of Figure 5 requires that the estimates in Table II of ($\delta_{ip} - \delta_{iq}$) be scaled upward and that of ($x - x'$) downward, about 40%, leading to a value near −0.04 for the latter. While the abscissas of the extrema in Figure 5 are not very sensitive to the value of α, the ordinates are, and a maximum value for ($x - x'$) of −0.04 corresponds to $\alpha \sim 0.2$, which is about two-thirds the value $(1 - 1/\sqrt{2}) = 0.293$ predicted by the simplest model for deuterium isotope effects on chemical equilibria.[11] There is still too much uncertainty in the magnitudes of the coefficients ($\delta_{ip} - \delta_{iq}$) to say precisely how close the correspondence is between

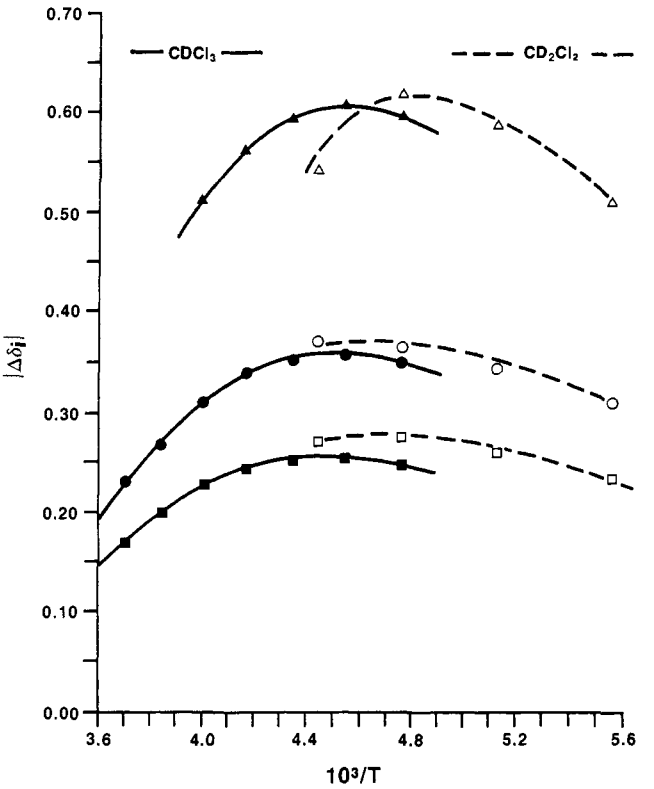

Figure 7. Temperature dependence of ^2H isotope shifts in compound **2''** along an abscissa proportionate to that in Figure 5, for (top to bottom) C7, C8, and C6. The solid curves for chloroform solution represent the least-squares fit to (5), neglecting the second term on its left-hand side, while the broken curves for methylene chloride solution are sketched.

Table III. Thermodynamic Values for the Equilibrium **2a''** ⇌ **2b''** (R = *n*-hexyl) in Chloroform Obtained by Fitting Eq 5 (λ_i Terms Omitted) to the Data in Figure 7

line	$-\Delta H$ (kcal mol^{-1})	ΔS (eu)
6	1.99 ± 0.06	−6.2 ± 0.2
7	1.94 ± 0.05	−6.1 ± 0.2
8	1.96 ± 0.04	−6.2 ± 0.2

theory and experiment, but it does appear that Hansen's proposal is not only empirically demonstrated but comes rather close to its very simplest theoretical approximation.

Assuming the theoretical value for α (which has small effect on the outcome), selecting lines for which the direct contributions, λ_{ip} and λ_{iq}, can be reasonably neglected, and fitting (5) to the data in Figure 7, one obtains the solid curves shown in the figure, and the thermodynamic values in Table III for the equilibrium **2a''** ⇌ **2b''** (*R* = *n*-hexyl) in chloroform solution. The rather large negative entropy of −6.2 eu is consistent with an increased constraint of the solvent by the separation of charge in the zwitterion. The solvent effects on the equilibria are, in retrospect, less clear than originally implied: they appear to be smaller in the *n*-alkyl systems than in **2'**, where the polar side chain seems to play an important role.[12]

4. General Discussion

The piroxicam system is a truly remarkable one by virtue of its tautomeric switches, which are readily thrown, and can change the dipole moment by amounts estimated to be of the order of 10 D.[14] The effects of different switch positions are exemplified by the variations in bond lengths summarized in Table IV, using the neutral 7,10 *EZE* form of piroxicam as a reference. The competition between charge separation and bond localization in the *N*-substituted pyridyl forms is reflected by the alternation of

(13) The upper limit of the measurable temperature range is determined by the onset of averaging with the small quantities of forms similar to **2c** and **2d** which are present in all samples.

(14) Reck, G.; Dietz, G.; Laban, G.; Gunther, W.; Bannier, G.; Hohne, E. *Die Pharmazie* **1988**, *43*(7), 477. This paper also describes a new crystalline form of neutral piroxicam.

Table IV. Bond Length Variations in Piroxicam Derivatives

bond	R: R′:	ref value[b] (7,10 *EZE*) H H	d′ − d(piroxicam)[a] 7′,10 *EZE*[c] H $-CH_3$	10 *ZZE*[d] H	10,16 *ZZZ*[e] H H	10,16′ *ZZE*[c] H *n*-hexyl	7,16′ *EZE*[d] H $-CH(CH_3)OCO_2Et$	7′,16′ *nZZ*[c,f] $-CH_3$ $-CH_3$
6,7		1.462		0.037	0.038	0.040		
7,8		1.369	−0.032	0.018	0.028	0.041		−0.031
8,9		1.463	0.036	−0.015	−0.032	−0.015		0.041
9,10		1.353		0.013	0.033	0.059	−0.015	−0.013
10,11		1.408		−0.014	−0.040	−0.051	−0.073	−0.065
11,12		1.386				0.027	0.030	0.028
12,13		1.380			−0.019	−0.020	−0.031	−0.019
13,14		1.360		0.011	0.025		0.035	0.011
14,15		1.375	−0.011		−0.019	−0.022	−0.043	−0.035
15,16		1.339			0.014		0.016	0.023
16,11		1.319	0.018	0.027	0.012	0.042	0.056	0.053

[a] Differences less than 0.01 A are omitted. [b] Reference 4. [c] Reference 2. [d] Section 5, this paper. [e] Reference 3. [f] Nonplanar due to ~90° rotation about 8,9 bond.

bond lengths within the pyridyl ring and the length of the 10,11 bond. Description of the system in terms of fully valence-bonded structures presents this issue too sharply; i.e., from the perspective of molecular orbital theory, all possible substitutions in Figure 1 involve the σ-electrons exclusively, the effect on the π-electron system being to alter the potential well near the substituted sites. Thus, by adding constant terms to the Coulomb integrals at the site of σ-substitution, all the trends in Table IV are reflected in the charge densities and π-bond orders at the simplest level of Huckel theory.

Nevertheless, the change in physical properties on switching to and from the formally zwitterionic 10,16 tautomers is profound, as indicated in Table III by the large entropy change, attributable to constraint of the solvent, accompanying this otherwise simple process. Conversely, the equilibrium is tunable over appreciable ranges by solvent and temperature. In this sense, the system not only has a switch but also a dimmer control attached to it. This has been used here to experimentally verify an explicated statement of Hansen's proposal that deuterium isotope shifts reflect the position of fast tautomeric equilibria and, in the process, establish close contact with the general theory of isotope effects for an especially simple case. If some of the structural features complicating this study (chirality, multiple rotamers) can be circumvented, systems modelled after this one should provide a versatile experimental approach to the study of fast tautomeric equilibria.

5. Experimental Section

NMR Spectra. The data in Table I and column 2 of Table II were obtained on a Bruker WM-250 spectrometer (2.5 cm bore) at a nominal ^{13}C frequency of 62.9 MHz, upgraded to include a pulse programmer, Aspect-3000 data system, and solid-state accessory. All other NMR measurements were conducted on an AM-500 spectrometer (126 MHz ^{13}C). In *N,N′*-dimethylformamide solution, the primary and secondary rate processes in **2′** were frozen out more or less concurrently at ~225 K, so that the spectra were assigned on the basis of an EXSY[15] experiment similar to that described in ref 5, aided by the prior assignments in Table I and the fact that shifts between members of the secondary pairs were generally smaller. The low temperature isotope shift measurements were corroborated by DEPT,[16] successive additions of small amounts of methanol-d_4 in order to track relative intensity changes, and by variations of the temperature. 32 K fids covering a spectral window of 30 000 Hz were zero-filled to 128 K, corresponding to a digital resolution of 0.003 ppm.

The CP/MAS spectrum was obtained from a ~100-mg sample packed into a 5-mm o.d. Maycor rotor with a PMMA stem, spun at 4.7 kHz, at a "magic angle" preset on a separate KBr sample. The 90° pulse width matching the Hartmann–Hahn condition was 3.3 μs, with a contact time of 4 ms and a relaxation delay of 4 s, and 1024 scans were accumulated.

Synthesis and Isolation of 2′: Carbonic Acid, 1-[1,2-Dihydro-2-[[(4-hydroxy-2-methyl-2*H*-1,2-benzothiazol-3-yl)carbonyl]imino]-1-pyridynyl]ethyl Ethyl Ester, *S,S*-Dioxide. A mixture of 30 g (0.09 mol) of piroxicam, 180 mL of acetone, 23.2 g (0.15 mol) of NaI, and 27.6 g (0.18 mol) of α-chlorodiethyl carbonate was stirred at reflux for 3.3 h. The acetone was stripped, and the residue was dissolved in 1.35 L of CH_2Cl_2, washed with aqueous bicarbonate and water, and stripped to solids. the solids were dissolved in 384 mL of hot acetone and diluted with 144 mL of water. The major product, 4-[1-((ethoxycarbonyl)-oxy)ethoxy]-2-methyl-*N*-(2-pyridyl)-2*H*-1,2-benzothiazine-3-carboxamide *S,S*-dioxide,[17] (26.9 g, 66%) was filtered, the mother liquor was extracted with CH_2Cl_2, and the extract was evaporated to leave a gum. The gum was subjected to column chromatography over silica gel using 4:1 CH_2Cl_2/EtOAc. Piroxicam and the major product above were first removed, followed by a yellow fraction which contained **2′**. Evaporation of this fraction yielded a solid which was titurated in Et_2O to give a yellow solid (0.75 g, 1.9%), mp 188–190 °C. Anal. Calcd for $C_{20}H_{21}N_3O_7S$: C, 53.69; H, 4.73; N, 9.39. Found: C, 53.61; H, 4.81; N, 9.18.

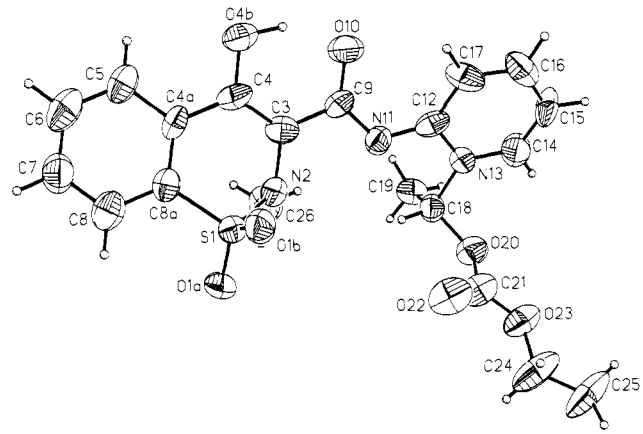

Figure 8. Crystal structure of compound **2c′**.

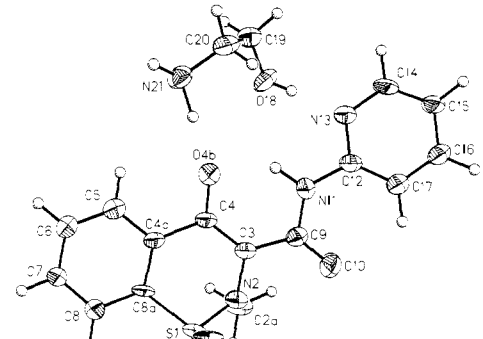

Figure 9. Crystal structure of ethanolamine salt of piroxicam. The third hydrogen on N21 is not visible in the drawing.

(15) Willem, R. *Prog. NMR Spectrosc.* **1987**, *20*, 1.
(16) Doddrell, D. M.; Pegg, D. T.; Bendall, M. R. *J. Magn. Reson.* **1982**, *48*, 323.
(17) U.S. Patent 4,551,452.

Table V. Single-Crystal X-ray Crystallographic Analysis

	compound 2c′	compound 4
A. Crystal Parameters		
formula	$C_{20}H_{23}N_3O_7S$ (449.5)	$C_{15}H_{13}N_3O_4S \cdot C_2H_7NO$ (392.4)
crystallization medium	dimethyl sulfoxide	acetonitrile
crystal size, mm	0.14 × 0.14 × 0.15	0.20 × 0.20 × 0.20
cell dimensions		
a =	10.018 (2) Å	12.823 (4) Å
b =	10.240 (3) Å	9.075 (4) Å
c =	11.351 (3) Å	9.954 (4) Å
α =	102.85 (2)°	123.01 (2)°
β =	110.71 (2)°	91.54 (3)°
γ =	93.16 (2)°	103.18 (3)°
V =	1050.4 (4) Å^3	929.5 (5) Å^3
space group	$P\bar{1}$	$P\bar{1}$
molecules/unit cell	2	2
density calcd, g/cm^3	1.42	1.40
linear absorptn factor, cm^{-1}	17.6	18.4
B. Refinement Parameters		
number of reflcns	2129	1921
nonzero reflcns ($I > 3.0\sigma$)	1359	1889
R index[a]	0.078	0.049
scale factor	1.694 (4)	0.750 (5)

[a] R index = $\sum||F_o| - |F_c||/\sum|F_o|$.

Crystal Structures. A representative crystal for each compound was surveyed, and a 1 A data set (maximum sin $\theta/\lambda = 0.5$) was collected on a Nicolet R3m/μ diffractometer for compound **2c′** and a Syntex P1 for compound **4**. Atomic scattering factors were taken from the International Tables for X-ray Crystallography.[18] All crystallographic calculations on **2c′** were facilitated by the SHELXTL[19] system, and those on **4** by the CRYM[20] system. All diffractometer data were collected at room temperature. Pertinent crystal, data collection, and refinement parameters are summarized in Table V.

In both cases, a trial structure was obtained by direct methods and refined routinely. Hydrogen positions were calculated wherever possible. The methyl hydrogens and hydrogen on oxygen were located by difference Fourier techniques. The hydrogen parameters were added to the structure factor calculations but were not refined. The shifts calculated in the final cycle of least-squares refinement were all less than 0.1 of their corresponding standard deviations. The final R index was 0.078 for compound **2c′** and 0.049 for compound **4**. The final difference Fouriers revealed no missing or misplaced electron density.

The refined structures were plotted (Figures 7 and 8) by using the SHELXTL plotting package. Coordinates, anisotropic temperature factors, distances, and angles are available as Supplementary Material (Tables S1-S10).

Acknowledgment. We gratefully acknowledge the substantial contributions of Andrew C. Braisted, who first isolated compound **2c′**, Diane Rescek, who conducted many of the NMR measurements, and Dr. B. W. Dominy, who performed the computations involved in Figure 7 and Table III.

Supplementary Material Available: Tables of atomic coordinates and isotropic thermal parameters (Table S1), bond lengths (Tables S2 and S7), bond angles (Tables S3 and S8), anisotropic thermal parameters (Table S4 and S9), H-atom coordinates and isotropic thermal parameters (Table S5), atomic coordinates (Table S6), and H-atom coordinates (Table S10) (10 pages). Ordering information is given on any current masthead page.

(18) (a) *International Tables for X-ray Crystallography*; Kynoch Press: Birmingham, 1974; Vol. IV, pp 55, 99, 149. (b) 1962; Vol. III, pp 204, 214.

(19) Sheldrick, G. M. SHELXTL User Manual, Nicolet Instrument Co., Madison, WI, 1981.

(20) Duchamp, D. J. American Crystallographers Associational Meeting, Paper B-14, Bozeman, MT, 1964; p 29.

Effect of Sequential Deuteriation upon the Solution Electron Affinity of Benzene

Gerald R. Stevenson,* Kerry A. Reidy, Steven J. Peters, and Richard C. Reiter

Contribution from the Department of Chemistry, Felmley 305, Illinois State University, Normal, Illinois 61761-6901. *Received January 30, 1989*

Abstract: The sequential addition of deuteriums to the six possible sites in benzene results in a nonlinear decrease in the solution EA, and this decrease in the EA is independent of the relative positions of substitution and thus orbital splitting. A plot of the reciprocal of the number of deuteriums vs $1/(1 - K)$, where K represents the equilibrium constant for electron transfer from the anion radical of the protiated benzene to the deuterium-substituted benzene, is exactly represented by a parabolic curve. This relationship has been linearized.

There are only two stable annulene anion radicals that are capable of maintaining the shape of a regular polyhedron on the ESR time scale. In both of these systems the odd electron is equally distributed between the doubly degenerate orbitals, which are nonbonding in the case of [8]annulene and antibonding in the case of [6]annulene. The presence of an electron-releasing substituent on the anion radical of [8]annulene results in a splitting of the degeneracy of the singly occupied nonbonding molecular orbitals, with a consequent increase in the spin density in the Ψ_{n+} MO at the expense of that in the Ψ_{n-}.[1] The relative increase in the spin density in Ψ_{n+} is due to the fact that the energy of this MO increases upon substitution, while that for Ψ_{n-} remains unperturbed (Figure 1A). In contrast to this, a single electron-releasing substituent on the [6]annulene anion radical results in a relative decrease in the spin density in the symmetric wave function (Ψ_s), which is increased in energy.[2] The antisymmetric wave function (Ψ_a) is unperturbed by the presence of an electron-releasing substituent (Figure 1B).

In the simplest model, the odd electron in the [8]annulene moiety or [6]annulene moiety can be described as existing in linear

(1) Stevenson, G. R.; Concepcion, J. G.; Echegoyen, L. *J. Am. Chem. Soc.* **1974**, *96*, 5452.

(2) Bolton, J. R.; Carrington, A.; Forman, A.; Orgel, L. E. *Mol. Phys.* **1962**, *5*, 43.

0002-7863/89/1511-6578$01.50/0